J Elast (2011) 104:105–114
DOI 10.1007/s10659-011-9317-6

Leading-Order Dynamics of Gravity-Driven Flows in Free-Standing Soap Films

Pinaki Chakraborty · Tuan Tran · Gustavo Gioia

Received: 30 November 2010 / Published online: 10 February 2011

Abstract We derive the leading-order equations that govern the dynamics of the flow in a falling, free-standing soap film. Starting with the incompressible Navier–Stokes equations, we carry out an asymptotic analysis using parameters that correspond to a common experimental setup. We account for the effects of inertia, surface elasticity, pressure, viscous stresses, gravity, and air drag. We find that the dynamics of the flow is dominated by the effects of inertia, surface elasticity, gravity, and air drag. We solve the leading-order equations to compute the steady-state profiles of velocity, thickness, and pressure in an experiment in which the film is in the Marangoni elasticity regime. The computational results, which include a Marangoni shock, are in good accord with the experimental measurements.

Keywords Soap films · Asymptotics

Mathematics Subject Classification (2000) 76A20 · 76M45

We dedicate this paper to the memory of Prof. Don Carlson, a gentleman and a scholar, a storied teacher and a sorely missed friend.

P. Chakraborty (✉)
Department of Geology, University of Illinois, Urbana, IL 61801, USA
e-mail: chakrabo@illinois.edu

T. Tran · G. Gioia
Department of Mechanical Science and Engineering, University of Illinois, Urbana, IL 61801, USA

T. Tran
e-mail: a.t.tran@utwente.nl

G. Gioia
e-mail: ggioia@illinois.edu

Present address:
T. Tran
Physics of Fluids Group, University of Twente, P.O. Box 217, 7500 AE, Enschede, The Netherlands

1 Introduction

A free-standing soap film consists of a bulk of fluid soapy solution sandwiched between two free surfaces [2]. The soap molecules on the free surfaces lessen the surface tension, make the film elastic, and stabilize the film. Because of their stability and thinness, free-standing soap films have long been used to study quasi-two-dimensional flows (see, e.g., [6]).

In the common experimental setup sketched in Fig. 1a, a free-standing soap film of average thickness H hangs between two long, vertical, mutually parallel wires a few centimeters apart from one another [5, 6, 9]. The film falls, driven by gravity, and a steady vertical flow of average velocity U soon becomes established within the bulk of the film. In a typical experiment, $H \approx 10\ \mu\text{m}$ and $U \approx 1$ m/s.

2 Equations

We restrict attention to the cross-section along the centerline of the film (Fig. 1). Thus, the flow resides in the x–y plane, and the independent variables are x, y, and the time t.

While the surfaces of water films tend to deform via antisymmetric modes (in which the two surfaces are in phase) [8], the surfaces of soap films preferentially deform via symmetric

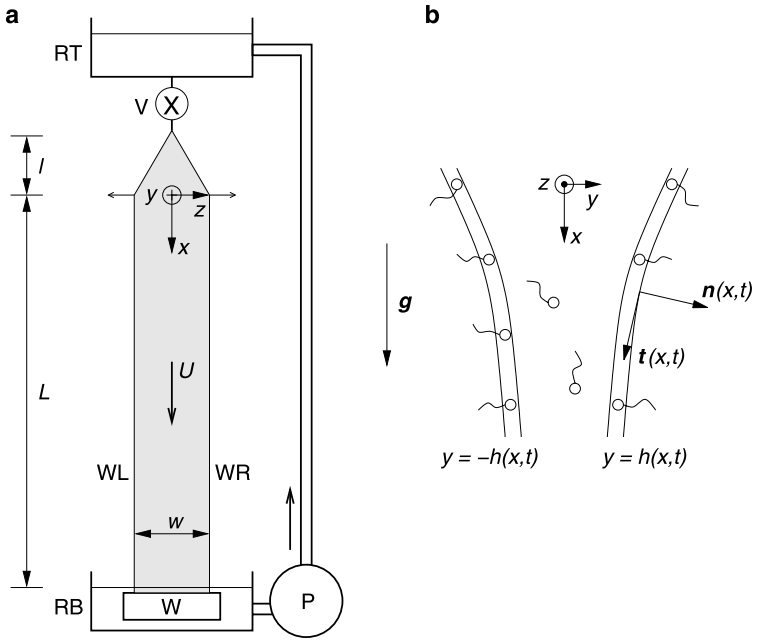

Fig. 1 (**a**) A common experimental setup used to study the flow in a falling, free-standing soap film [5, 6, 9]. Wires WL and WR are thin nylon-fishing lines kept taut by weight W. The film hangs from the wires; its width increases from 0 to W over an expansion section of length l, then remains constant and equal to W over a measurement section of length L. Reservoir RT contains a soapy solution which flows through valve V and into the film. After flowing through the film with average vertical velocity U, the soapy solution drains into reservoir RB and returns to reservoir RT via pump P. In a typical experiment, the soapy solution consists of $\approx 2.5\%$ Dawn Nonultra in water; $W \approx 5$ cm; $L \approx 1$ m; and $l \approx 10$ cm. (**b**) The cross-section along the centerline of the film. The surfaces of the film are located at $y = \pm h(x,t)$; the film thickness is $2h(x,t)$. The vectors $\boldsymbol{n}(x,t)$ and $\boldsymbol{t}(x,t)$ denote the normal and tangent vectors, respectively, at the film surface $y = h(x,t)$

modes (in which the two surfaces mirror each other) [2]. Therefore, we assume that the surfaces of the film remain symmetric with respect to the x-axis, and are located at $y = \pm h(x,t)$ (Fig. 1b). These surfaces provide the boundary conditions for the bulk flow.

2.1 Dimensional Equations

We begin by considering the bulk flow, which obeys the incompressible Navier–Stokes equations:

$$\nabla \cdot \boldsymbol{u} = 0, \tag{1}$$

$$\rho \frac{D\boldsymbol{u}}{Dt} = -\nabla p + \mu \nabla^2 \boldsymbol{u} + \rho \boldsymbol{g}. \tag{2}$$

Here $\boldsymbol{u} = (u, v)$ is the velocity vector, $u = u(x, y, t)$ and $v = v(x, y, t)$ are respectively the vertical and horizontal component of $\boldsymbol{u}$, ρ is the density of the fluid, $D/Dt \equiv \partial/\partial t + \boldsymbol{u} \cdot \nabla$ is the substantial derivative, $p(x, y, t)$ is the pressure in the film, μ is the dynamic viscosity of the fluid, and $\boldsymbol{g} = (g, 0)$ is the gravitational acceleration. Equation (1) represents the conservation of mass. Equation (2) represents the conservation of momentum—the dynamic balance of inertia, pressure, viscous stresses, and gravity. Note that we do not consider the drag of the wires because it is negligible as compared with the air drag [5].

A fluid element on the film surface at $y = h$ is subjected to a force due to the bulk flow (pressure and viscous stresses), a force due to the ambient air (atmospheric pressure and air drag), and a force due to the surface elasticity (surface tension and its gradient). The force balance, which sets the dynamic boundary condition [1, 3, 4] at $y = h$, reads:

$$\begin{aligned} -(p - p_a) + \boldsymbol{n} \cdot \mu(\nabla \boldsymbol{u} + \nabla \boldsymbol{u}^T) \cdot \boldsymbol{n} &= \kappa \sigma, \\ \boldsymbol{t} \cdot \mu(\nabla \boldsymbol{u} + \nabla \boldsymbol{u}^T) \cdot \boldsymbol{n} + \tau_a &= \boldsymbol{t} \cdot \nabla_s \sigma, \end{aligned} \tag{3}$$

where the balance is expressed along the normal to the surface and along the tangent to the surface, respectively. (Refer to the Appendix for details of the notation and derivation.) Further, the film surface at $y = h$ has to satisfy the kinematic boundary condition:

$$v = \frac{\partial h}{\partial t} + u \frac{\partial h}{\partial x}. \tag{4}$$

Finally, symmetry of the film surfaces about the x-axis imposes the following conditions at $y = 0$:

$$\begin{aligned} v &= 0, \\ \frac{\partial u}{\partial y} &= 0. \end{aligned} \tag{5}$$

Equations (1)–(5) are not complete without models of the surface elasticity and the air drag. First, consider the surface elasticity. The deformation of the surfaces of the film may disturb the mutual equilibrium between the soap molecules in the bulk and the soap molecules on the surfaces, causing the diffusion of soap molecules between the bulk and the surfaces. The concentration of the soap molecules on the surfaces determines the surface tension σ, whose variation with the thickness of the film is related with the elastic modulus of the film, E, in the form [2]:

$$\frac{d\sigma}{dh} = -\frac{E}{2h}. \tag{6}$$

In general, modeling the diffusion of the soap molecules between the bulk and the surfaces entails consideration of additional governing equations [1]. Nevertheless, in the experimental setup of Fig. 1a there is insufficient time for such a diffusion to occur [9]. Thus, the concentration of soap molecules in the bulk remains constant, and the film is said to be in the "Marangoni elasticity regime," one of two possible limit regimes. (Refer to the Appendix for a discussion of the other limit regime: the "Gibbs elasticity regime.") In the Marangoni regime, the speed of the elastic waves, called the Marangoni speed and denoted U_M, is a property of the film, independent of h. This is the speed at which disturbances in h travel on the surfaces of the film. (In the experimental setup of Fig. 1a, U_M and U are of comparable magnitude [9].) The relation between the Marangoni speed U_M and the Marangoni elastic modulus E_M, $U_M = \sqrt{(E_M/2\rho h)}$, allows us to rewrite equation (6) in the form:

$$\frac{\partial \sigma}{\partial x} = -\rho U_M^2 \frac{\partial h}{\partial x}. \tag{7}$$

Next, consider the air drag. The film can be thought of as a flat plate that moves with velocity u. Assuming that the air flow is laminar, the shear stress on one surface of the film can be calculated using Blasius's solution for a boundary layer [7], resulting in the following expression:

$$\tau_a = \alpha_a \sqrt{\rho_a \mu_a} \sqrt{\frac{u^3}{x+1}}, \tag{8}$$

where ρ_a and μ_a are respectively the density and the viscosity of the ambient air. The constant α_a can be calculated numerically from the Blasius boundary layer equation. (We will use $\rho_a = 1.2$ kg/m^3, $\mu_a = 1.7 \times 10^{-5}$ kg/ms, and $\alpha_a = 0.3$.)

In the analysis that follows, we need not invoke any explicit models for the surface elasticity and the air drag, and limit ourselves to note that in dimensionless variables the surface elasticity and the air drag are $O(1)$.

2.2 Dimensionless Equations

The soap film has a typical length $L \approx 1$ m and an average thickness $H \approx 10$ μm (Fig. 1a). We introduce the small dimensionless parameter $\epsilon = H/L \approx 10^{-5}$ and, following Chomaz [1], we invoke the principle of dominant balance to relate the dimensionless variables (denoted with primes) to their dimensional counterparts:

$$\begin{aligned} x &= Lx', \qquad y = Hy', \\ u &= Uu', \qquad v = \epsilon U v', \\ h &= Hh', \qquad t = \frac{L}{U} t', \\ p &= p_a + \frac{\mu U}{L} p', \qquad \sigma = \sigma_m + \rho H U^2 \sigma', \end{aligned} \tag{9}$$

where U is the average vertical velocity and σ_m is the average surface tension of the film. Since U and U_M are of comparable magnitudes, the expression $\sigma = \sigma_m + \rho H U^2 \sigma'$ is consistent with the surface elasticity model of (7). Note that we have departed from Chomaz in assuming that the pressure is in balance with the viscous stresses. We shall show that the leading-order pressure term that follows from this assumption is consistent with the symmetry of the film surfaces—the leading-order transverse pressure gradient is zero [1].

The governing equations (1)–(2) read (in the dimensionless variables, from which we drop the primes for simplicity of notation):

$$\frac{\partial u}{\partial x}+\frac{\partial v}{\partial y}=0, \tag{10}$$

$$\epsilon \mathrm{Re}\frac{Du}{Dt}=-\epsilon^2\frac{\partial p}{\partial x}+\epsilon^2\frac{\partial^2 u}{\partial x^2}+\frac{\partial^2 u}{\partial y^2}+\epsilon\frac{\mathrm{Re}}{\mathrm{Fr}}, \tag{11}$$

$$\epsilon \mathrm{Re}\frac{Dv}{Dt}=-\frac{\partial p}{\partial y}+\epsilon^2\frac{\partial^2 v}{\partial x^2}+\frac{\partial^2 v}{\partial y^2}, \tag{12}$$

where $\mathrm{Re}\equiv\rho U H/\mu$ is the Reynolds number and $\mathrm{Fr}\equiv U^2/(gL)$ is a Froude-like number.

Neglecting terms of $O(\epsilon^2)$, the dynamic boundary conditions at $y=h$ (equations (3)) read (in the dimensionless variables, from which we again drop the primes for simplicity of notation):

$$\begin{aligned} p+\epsilon\frac{\partial^2 h}{\partial x^2}\left(\mathrm{Ca}^{-1}+\mathrm{Re}\,\sigma\right)&=2\left(\frac{\partial v}{\partial y}-\frac{\partial u}{\partial y}\frac{\partial h}{\partial x}\right),\\ \epsilon\mathrm{Re}\frac{\partial \sigma}{\partial x}&=\frac{\partial u}{\partial y}+\epsilon\mathrm{D}, \end{aligned} \tag{13}$$

where $\mathrm{Ca}\equiv\mu U/\sigma_m$ is the capillary number and $\mathrm{D}\equiv\tau_a L/(\mu U)$ is the dimensionless air drag. The kinematic boundary condition at $y=h$ (equation (4)) and the symmetry conditions at $y=0$ (equations (5)) remain unchanged in the dimensionless variables.

3 Asymptotics

We are now ready to obtain the equations governing the leading-order dynamics. We expand the fields (u, v, p, h, σ) in a power series of ϵ of the generic form:

$$f=f_0+\epsilon f_1+O(\epsilon^2). \tag{14}$$

We substitute the expansions in the governing equations, boundary conditions, and symmetry conditions of Sect. 2.2. In Table 1 we list the magnitudes of the relevant quantities. Noting that all the dimensionless numbers are of $O(\epsilon^0)$, we proceed to writing the equations at different orders of ϵ.

3.1 Leading-Order Equations

The governing equations at $O(\epsilon^0)$ read:

$$\frac{\partial u_0}{\partial x}+\frac{\partial v_0}{\partial y}=0, \tag{15}$$

$$\frac{\partial^2 u_0}{\partial y^2}=0, \tag{16}$$

$$-\frac{\partial p_0}{\partial y}+\frac{\partial^2 v_0}{\partial y^2}=0. \tag{17}$$

Table 1 Estimates of parameters, characteristic quantities, and dimensionless numbers for soap-film flows in the experimental setup of Fig. 1a. To estimate the magnitude of D, we note that $u \sim U$ and $x \sim L$; from $\mathrm{D} \equiv \tau_a L/(\mu U)$ and (8), we find $\mathrm{D} \approx 10^0$

Parameters	Symbol	Estimate
Viscosity of soapy solution	μ	$\approx 10^{-3}$ kg/(m s)
Density of soapy solution	ρ	≈ 1000 kg/(m^3)
Average surface tension	σ_m	$\approx 10^{-2}$ kg/s^2
Characteristic quantities		
Film length	L	≈ 1 m
Average film thickness	H	$\approx 10^{-5}$ m
Average vertical velocity	U	≈ 1 m/s
Dimensionless numbers		
Asymptotic parameter	ϵ	10^{-5}
Reynolds number	Re	10^1 $[O(\epsilon^0)]$
Froude number	Fr	10^{-1} $[O(\epsilon^0)]$
Capilliary number	Ca	10^{-1} $[O(\epsilon^0)]$
Air Drag	D	10^0 $[O(\epsilon^0)]$

The boundary conditions at $y = h$ read:

$$\begin{aligned} p_0 &= 2\frac{\partial v_0}{\partial y} - 2\frac{\partial u_0}{\partial y}\frac{\partial h_0}{\partial x}, \\ \frac{\partial u_0}{\partial y} &= 0, \\ v_0 &= \frac{\partial h_0}{\partial t} + u_0\frac{\partial h_0}{\partial x}. \end{aligned} \tag{18}$$

The symmetry conditions at $y = 0$ read:

$$\begin{aligned} \frac{\partial u_0}{\partial y} &= 0, \\ v_0 &= 0. \end{aligned} \tag{19}$$

This set of equations can be simplified to the following:

$$\begin{aligned} u_0 &= u_0(x,t), \\ \frac{\partial h_0}{\partial t} + \frac{\partial u_0 h_0}{\partial x} &= 0, \\ v_0 &= -\frac{\partial u_0}{\partial x}y, \\ p_0 &= -2\frac{\partial u_0}{\partial x}. \end{aligned} \tag{20}$$

We find that the leading-order terms u_0 and p_0 are uniform across the thickness. The leading-order transverse pressure gradient, $\partial p_0/\partial y$, is zero, as required by the symmetry of the film surfaces [1].

Note that h_0, v_0, and p_0 are expressed in terms of u_0, but u_0 remains undetermined. To determine u_0 (and the velocity, pressure, and thickness fields) to the leading order, we turn next to the $O(\epsilon)$ equations.

3.2 $O(\epsilon)$ Equations

To obtain the equations for the leading-order terms, it is necessary to consider only the following $O(\epsilon)$ equations. The governing equation for x-momentum at $O(\epsilon)$ reads:

$$\mathrm{Re}\frac{Du_0}{Dt} = \frac{\partial^2 u_1}{\partial y^2} + \frac{\mathrm{Re}}{\mathrm{Fr}}. \tag{21}$$

Integrating this equation in y and applying the following symmetry condition at $y = 0$:

$$\frac{\partial u_1}{\partial y} = 0, \tag{22}$$

we get:

$$\frac{\partial u_1}{\partial y} = -\frac{\mathrm{Re}}{\mathrm{Fr}} y + \mathrm{Re}\, y \left(\frac{\partial u_0}{\partial t} + u_0 \frac{\partial u_0}{\partial x} \right), \tag{23}$$

where we have used the leading-order solution $u_0 = u_0(x, t)$. Eliminating $\partial u_1/\partial y$ between equation (23) and the following boundary condition at $y = h$:

$$\mathrm{Re}\frac{\partial \sigma_0}{\partial x} = \frac{\partial u_1}{\partial y} + \mathrm{D}, \tag{24}$$

we get:

$$\mathrm{Re}\, h_0 \left(\frac{\partial u_0}{\partial t} + u_0 \frac{\partial u_0}{\partial x} \right) = \frac{\mathrm{Re}}{\mathrm{Fr}} h_0 + \mathrm{Re}\frac{\partial \sigma_0}{\partial x} - \mathrm{D}. \tag{25}$$

4 Results and Discussion

We are now ready to write the leading-order equations, which we write in the dimensional form. Equation (25) in dimensional form reads:

$$\rho h_0 \left(\frac{\partial u_0}{\partial t} + u_0 \frac{\partial u_0}{\partial x} \right) = \frac{\partial \sigma_0}{\partial x} + \rho g h_0 - \tau_a. \tag{26}$$

This is the leading-order equation for u_0 and shows that the flow is dominated by the forces of inertia, surface elasticity, gravity, and air drag. Note that had we expanded the air drag as a field, τ_a in the above equation would be the leading-order term of the expansion. The leading-order equations for the other fields can be obtained by writing equations (20) in dimensional form:

$$\frac{\partial h_0}{\partial t} + \frac{\partial u_0 h_0}{\partial x} = 0, \tag{27}$$

$$v_0 = -\frac{\partial u_0}{\partial x} y, \tag{28}$$

$$p_0 = p_a - 2\mu \frac{\partial u_0}{\partial x}. \tag{29}$$

In Fig. 2 we show the representative steady-state profiles of $u_0(x), h_0(x), v_0(x)$, and $p_0(x)$ corresponding to the experimental setup of Fig. 1a. These profiles, computed by

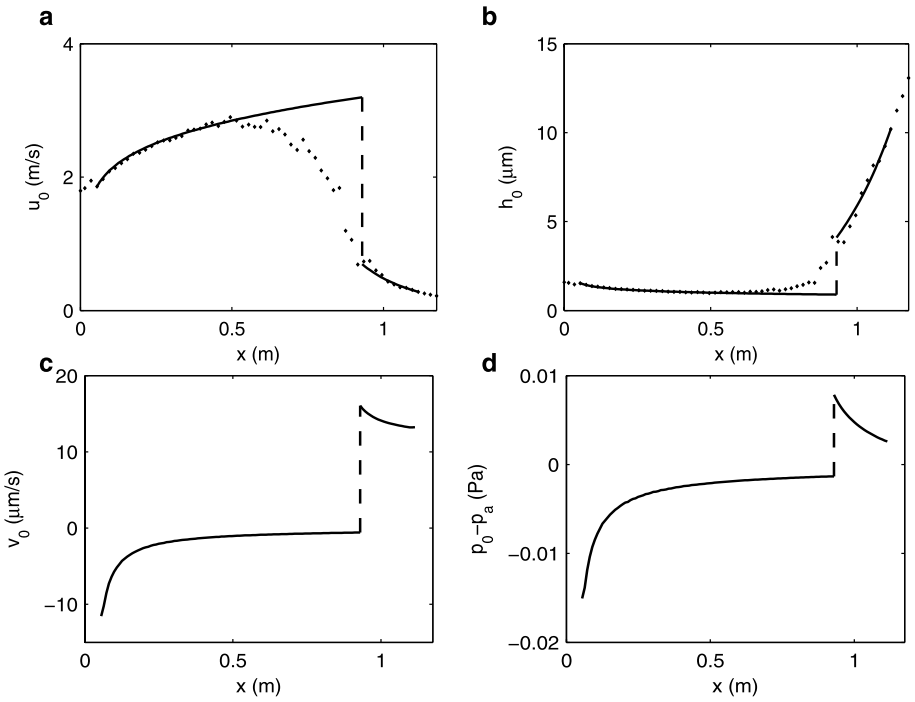

Fig. 2 Steady-state profiles (shown as solid lines) of (**a**) $u_0(x)$, (**b**) $h_0(x)$, (**c**) $v_0(x)$ at $y = h_0(x)$, and (**d**) $p_0(x)$ corresponding to the experimental setup of Fig. 1a with length $L = 1.17$ m, width $W = 5.1$ cm, Marangoni speed $U_M = 1.48$ m/s, and flux $q = 5.7 \times 10^{-6}$ m^2/s. In the steady state $u_0(x)h_0(x)$ is constant and equal to $q/2$ (equation (27)). We compute the profile $u_0(x)$ by solving equation (26) with suitable boundary conditions upstream and downstream of the measurement section of the soap film (Fig. 1a), namely the experimentally measured values of $u_0(x = W)$ and $u_0(x = L - W)$. (We do not impose the boundary conditions at $x = 0$ and $x = L$ because the experimentally measured values of $u_0(x = 0)$ and $u_0(x = L)$ may be affected by end effects.) The value of $u_0(x = W)$ is set by the opening of the valve V and the value of $u_0(x = L - W)$ is set by the dynamics of the film draining into the reservoir RB (Fig. 1a). The Marangoni shock is represented with a dashed line; its location is determined using the Rayleigh's jump condition, $u_{0+}u_{0-} = U_M^2$, where the subscripts $+$ and $-$ denote downstream and upstream of the shock, respectively [9]. Using the solution $u_0(x)$ we compute the other fields by solving equations (27)–(29). The experimental data points $u(x)$ (panel a) were measured using Laser Doppler Velocimetry, and are taken from [9]. The data points $h(x)$ (panel b) are computed from the data points $u(x)$ using the relation $h(x) = q/2u(x)$. $v(x)$ and $p(x)$ were not measured experimentally

solving the leading-order equations (26)–(29) coupled with the models of surface elasticity (equation (7)) and air drag (equation (8)), are in good accord with experimental measurements. (For an extensive comparison with the experiments, refer to [9].) In particular, the equations provide a suitable framework for elucidating a striking experimental observation: a Marangoni shock [9]. In the profile of $u_0(x)$ (Fig. 2a), the film velocity does not increase monotonically downstream, as it is widely thought. Instead the velocity increases, peaks, drops abruptly, then lessens gradually downstream. The equations reveal that the abrupt drop in velocity is caused by a shock related to the surface elasticity—a Marangoni shock which marks the transition from a supercritical region (where $u_0(x) > U_M$) to a subcritical region (where $u_0(x) < U_M$). Although the equations predict a sharp shock, the shock observed experimentally is diffused over a finite width (Fig. 2a). The shock dissipates energy

by powering locally intense turbulent fluctuations [9]. These locally intense turbulent fluctuations (which are not taken into account in our equations) endow the shock with a finite width, which could be predicted by adding a suitable diffusive term to our equations.

To summarize, by employing the principle of dominant balance (equations (9)) and asymptotic expansions in power series of ϵ, we have obtained the leading-order equations for the velocity, thickness, and pressure fields along the centerline of a free-standing, falling soap film.

Acknowledgements This work was financially supported by the US National Science Foundation through NSF/DMR grant 10–44901 (Daniele Finotello, program director). PC acknowledges support from the Roscoe G. Jackson II research fellowship. TT acknowledges support from the Vietnam Education Foundation.

Appendix

Dynamic Boundary Condition on Surfaces of the Film

Consider the surface of the film at $y = h(x,t)$. We denote the curvature of this surface by $\kappa(x,t)$. The normal vector to the surface, $\boldsymbol{n}$, points outward and the tangent vector, $\boldsymbol{t}$, is parallel to the velocity of the fluid at the surface (see Fig. 1b). The surface vectors and curvature can be calculated as follows:

$$\boldsymbol{n} = \frac{1}{\left(1+\left(\frac{\partial h}{\partial x}\right)^2\right)^{1/2}}\left(-\frac{\partial h}{\partial x}, 1\right), \tag{30}$$

$$\boldsymbol{t} = \frac{1}{\left(1+\left(\frac{\partial h}{\partial x}\right)^2\right)^{1/2}}\left(1, \frac{\partial h}{\partial x}\right), \tag{31}$$

$$\kappa = \frac{\frac{\partial^2 h}{\partial x^2}}{\left(1+\left(\frac{\partial h}{\partial x}\right)^2\right)^{3/2}}. \tag{32}$$

We now outline the standard approach for computing the dynamic boundary condition at the surface (see, e.g., [1, 3, 4]). The dynamic boundary condition is a statement of the force balance for a fluid element on the surface. This element is subjected to the following forces. First, the force due to the bulk flow:

$$\boldsymbol{f}_b = -p\boldsymbol{n} + \mu(\nabla\boldsymbol{u} + \nabla\boldsymbol{u}^T)\cdot\boldsymbol{n}. \tag{33}$$

Second, the force due to the ambient air:

$$\boldsymbol{f}_a = -p_a\boldsymbol{n} - \tau_a\boldsymbol{t}, \tag{34}$$

where p_a is the atmospheric pressure and τ_a is the frictional shear stress or air drag that the surface experiences as it rubs against the ambient air. Last, the force due to the surface elasticity:

$$\boldsymbol{f}_e = \kappa\sigma\boldsymbol{n} + \nabla_s\sigma, \tag{35}$$

where $\nabla_s = \nabla - \boldsymbol{n}(\boldsymbol{n}\cdot\nabla)$ is the surface gradient operator.

The force balance equation for the surface reads:

$$\boldsymbol{f}_b = \boldsymbol{f}_a + \boldsymbol{f}_e. \tag{36}$$

On rearrangement of this equation, we obtain the dynamic boundary condition at $y = h$:

$$-(p - p_a)\boldsymbol{n} + \mu(\nabla \boldsymbol{u} + \nabla \boldsymbol{u}^T) \cdot \boldsymbol{n} + \tau_a \boldsymbol{t} = \kappa\sigma \boldsymbol{n} + \nabla_s \sigma. \tag{37}$$

By projecting equation (37) on the normal vector $\boldsymbol{n}$ and on the tangent vector $\boldsymbol{t}$, we obtain equations (3).

Gibbs Elasticity Regime

The Marangoni elasticity regime governs the dynamics of the film for short time scales, where there is insufficient time for the soap molecules to diffuse between the bulk and the surfaces. For long time scales, where the soap molecules in the bulk and the soap molecules on the surfaces remain in thermodynamic equilibrium, the film is in the Gibbs elasticity regime. The Gibbs elastic modulus E_G can be expressed in the form [2]:

$$E_G = 2RTc\frac{h}{(1 + h/k)^2}, \tag{38}$$

where R is the gas constant, T is the absolute temperature, c is the overall concentration of soap molecules in the film, and k is the constant that characterizes the thermodynamic equilibrium between the soap molecules in the bulk and the soap molecules on the surfaces. The speed of the corresponding elastic waves, the Gibbs speed U_G is related with E_G via $U_G = \sqrt{(E_G/2\rho h)}$. Note that unlike the Marangoni speed, the Gibbs speed depends on h.

References

1. Chomaz, J.M.: The dynamics of a viscous soap film with soluble surfactant. J. Fluid Mech. **442**, 387–409 (2001)
2. Couder, Y., Chomaz, J.M., Rabaud, M.: On the hydrodynamics of soap films. Physica D **37**(1–3), 384–405 (1989)
3. Craster, R.V., Matar, O.K.: Dynamics and stability of thin liquid films. Rev. Mod. Phys. **81**(3), 1131–1198 (2009)
4. Oron, A., Davis, S.H., Bankoff, S.G.: Long-scale evolution of thin liquid films. Rev. Mod. Phys. **69**(3), 931–980 (1997)
5. Rutgers, M.A., Wu, X.L., Bhagavatula, R., Petersen, A.A., Goldburg, W.I.: Two-dimensional velocity profiles and laminar boundary layers in flowing soap films. Phys. Fluids **8**, 2847–2854 (1996)
6. Rutgers, M.A., Wu, X.L., Daniel, W.B.: Conducting fluid dynamics experiments with vertically falling soap films. Rev. Sci. Instrum. **72**, 3025–3037 (2001)
7. Schlichting, H., Gersten, K., Gersten, K.: Boundary-Layer Theory. Springer, Berlin (2000)
8. Taylor, G.I.: The dynamics of thin sheets of fluid. II. Waves on fluid sheets. Proc. R. Soc. Lond. A **253**(1274), 296–312 (1959)
9. Tran, T., Chakraborty, P., Gioia, G., Steers, S., Goldburg, W.: Marangoni shocks in unobstructed soap-film flows. Phys. Rev. Lett. **103**(10), 104501 (2009)